

## Photoelectron spectroscopy of the laser-excited $\bar{X}$ surface state on GaAs(110) using synchrotron radiation

J. P. Long, S. S. Goldenberg, and M. N. Kabler

Naval Research Laboratory, Washington, D.C. 20375

(Received 16 September 1992)

An excited surface state on GaAs(110) has been investigated using a technique which populates the state with a laser pulse and measures its properties by time-resolved photoelectron spectroscopy using synchrotron radiation. Measurements of momentum, energy, and lifetime show that this is an intrinsic surface state near  $\bar{X}$  in the surface Brillouin zone which equilibrates with bulk conduction electrons during the 5-ns pump pulse. The narrow photoelectron band increases linearly in kinetic energy with the probe photon energy, and no final-state effects appear in the limited energy range investigated.

Excited electronic states on the surfaces of semiconductors are involved in a variety of phenomena including surface recombination, photovoltage, adsorbate bonding, epilayer growth, and surface photochemical reactions. Photoelectron spectroscopy (PES) using fixed-frequency lasers has proved to be a fruitful approach for investigating laser-excited states from a variety of group-IV,<sup>1,2</sup> III-V,<sup>3,4</sup> and II-VI (Ref. 5) semiconductors. However, this technique is limited in probe wavelength and tunability. In order to broaden the array of available tools, we have performed the first set of PES experiments which uses pulses of continuously tunable photons from a synchrotron radiation (SR) source as a probe of normally unoccupied semiconductor states populated by pulsed laser excitation. The primary object was a previously well-characterized<sup>3</sup> state on cleaved GaAs(110) with energy near the conduction-band minimum (CBM) and wave vector at  $\bar{X}$  in the surface Brillouin zone (BZ). Despite the low number of SR photons ( $\sim 10^4$ ) in the monochromatic probe pulse, we have been able to resolve both the momentum and lifetime of the  $\bar{X}$  state. The kinetic energy of the narrow band of photoelectrons from  $\bar{X}$  increases linearly with probe energy  $h\nu$  in the range  $8 \leq h\nu \leq 12$  eV, consistent with the simple concept of photoemission from a narrow surface state into vacuum. The photoemission efficiency shows no evidence, within fairly wide latitude, of variation of the character of the final state with  $h\nu$ . The  $\bar{X}$  population decays in approximately 1 ns and is consistent with equilibrium between  $\bar{X}$  and conduction electrons near the surface.

The normally unoccupied state at  $\bar{X}$  has been identified both by laser excite-and-probe, angle-resolved photoemission spectroscopy (ARPES),<sup>3</sup> and by inverse photoemission spectroscopy.<sup>6</sup> A first-principles quasiparticle band structure calculated for the relaxed GaAs(110) surface indicates that the  $\bar{X}$  state represents an absolute minimum in the lowest unoccupied surface band.<sup>7</sup> The excited-state ARPES used a 1.78-eV pump photon and 10.72-eV probe and found a laser-populated state at or near  $\bar{X}$  and within about 0.1 eV of the CBM. Time-delay experiments with subpicosecond resolution established that the state was populated indirectly, either by electrons scattered from states near the center of the surface BZ (Ref.

3) or from the bulk.<sup>7</sup>

It is advantageous to probe electronic states with a tunable photon in order to examine final-state effects and to investigate resonances. SR not only provides tunability but also gives access to core levels which, as we illustrate below, can provide important information for interpreting excited-state spectra from surfaces with nonuniform equilibrium band bending. Two primary problems with SR as a probe of laser-excited states are the background of photoelectrons excited by higher-order or scattered light in the monochromatized SR beam and the mismatch between the repetition rates of many lasers and the SR pulses. For these initial experiments, the background was eliminated by inserting a LiF filter into the SR beam, albeit at a significant cost in tuning range. The pulse-rate mismatch was minimized by using the high repetition rate of a copper vapor laser, which produced 5-ns, 2.43-eV pulses at 6 kHz, and also by exploiting the reduced SR pulse rate (1.76 MHz) available during single-bunch operation at the National Synchrotron Light Source, Brookhaven (beam line X24C). The laser was synchronized to the storage ring and timing electronics insured that photoelectron energy distribution curves (EDC's) were accumulated only from SR pulses (0.5-ns pulse duration) coincident with the laser pulse to within a controllable relative delay.<sup>8</sup> A double-pass cylindrical mirror analyzer (CMA) was used for photoelectron energy analysis. An energy resolution (CMA plus monochromator) of  $180 \pm 20$  meV was determined from the Fermi edge of gold. GaAs bars were secured with indium to a water-cooled stage and cleaved *in situ* at pressures below  $2 \times 10^{-10}$  torr. The peak temperature at the 2-mm-diameter laser spot was held between 296 and 304 K.

Figure 1 compares EDC's in the region around the band gap for samples oriented as in Fig. 2(a). The open points in Fig. 1 were recorded during the laser pulse. The band at 0.06 eV for *n*-type and 1.26 eV for *p*-type samples arises from electrons excited by the 0.6-mJ/cm<sup>2</sup> laser pulse into the surface-state minimum near  $\bar{X}$ . For reference, the amplitude of the  $\bar{X}$  signal, which is linear in laser fluence up to the maximum (6 mJ/cm<sup>2</sup>) investigated, is  $\sim 0.03\%$  of the valence-band amplitude.

Although just after cleavage the bands were usually flat

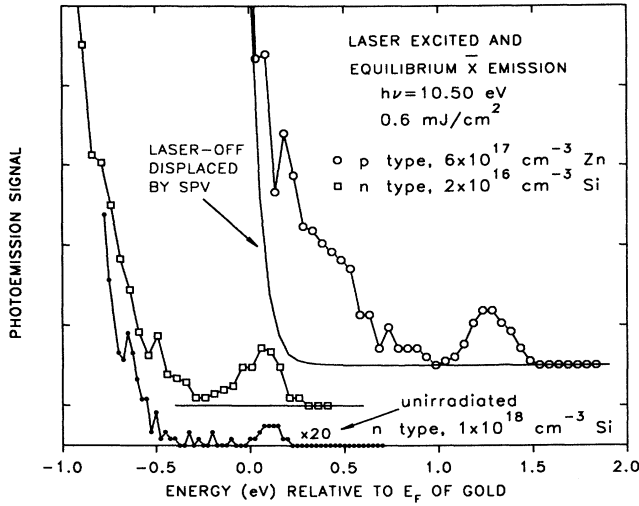


FIG. 1. EDC's of the band-gap region recorded during the laser pulse (open symbols), between laser pulses (solid line), and in equilibrium (solid symbols). EDC's are offset vertically for clarity.

to within 0.1 eV, as expected for normal cleaves of GaAs, laser exposure created nonuniform band bending over our surfaces.<sup>9</sup> During a laser pulse, however, the surface photovoltage (SPV) (Ref. 10) effectively flattened the bands uniformly.<sup>11</sup> The separation  $\Delta E$  of the peaks in Fig. 1 measures the extent of band flattening in the regions contributing to the  $\bar{X}$  signal. For flat bands,  $\Delta E = \Delta E_f$ , where  $\Delta E_f$  is the difference between bulk Fermi levels in the  $n$ - and  $p$ -type samples, as measured with respect to a band edge. Since in Fig. 1  $\Delta E_f = 1.27$  and  $\Delta E = 1.20$  eV, we conclude that the bands are nearly flat within experi-

mental accuracy. The EDC's along with the known  $E_f$  values then determine the energy of the occupied  $\bar{X}$  minimum to be within 0.1 eV of the CBM, in agreement with prior work.<sup>3</sup>

On  $n$ -type samples with relatively high doping levels and small band bending, the  $\bar{X}$  state is sufficiently close to  $E_f$  to be populated in the dark. This is the likely origin of the weak equilibrium peak near 0.1 eV in the lowest EDC of Fig. 1. The EDC was recorded prior to laser exposure and in the geometry of Fig. 2(a), which excludes any direct emission from  $\bar{\Gamma}$ . The energy of this peak adds further support to the conclusion that the occupied  $\bar{X}$  minimum is very near the CBM. One would wish to calibrate the density of the laser-excited  $\bar{X}$  population with this equilibrium signal, but the result depends too strongly on its energy relative to  $E_f$ .

Several types of extrinsic state contribute to the photoemission which appears within the band gap during the laser pulse. The identification of these states is complicated by the presence of inhomogeneous band bending in the dark, which leads to spatially varying SPV shifts during the laser pulse. For example, consider one specific source of gap emission, metallic Ga islands ( $\sim 100$ -Å diameter) formed through the laser-induced photochemical decomposition of the surface.<sup>9</sup> A prominent Fermi edge from these islands is evident in EDC's measured for  $n$ -type samples in equilibrium after sufficient laser exposure.<sup>12</sup> However, as is evident from the laser-off EDC in Fig. 1, island emission for  $p$ -type samples is obscured by the strong valence emission unless the EDC is recorded during a laser pulse. It has been established from time-resolved Ga 3d line shapes that, when the bands are uniformly flattened during a laser pulse, the SPV shift  $\Delta V$  of Ga islands exceeds that of the substrate by several tenths of an eV.<sup>9</sup> Thus, during a laser pulse the Fermi edge of the Ga islands appears in the spectrum at an energy  $E_f + \Delta V$ . This shifts the island emission above the valence-band edge, where it mimics laser-excited defect states. It is interesting to speculate whether similar effects might have contributed to the gap signals in earlier studies of laser-excited GaAs which had been dosed with oxygen and with gold.<sup>13</sup>

Other equilibrium-occupied defect states associated with either cleavage- or laser-induced defects may also contribute to the gap emission seen in Fig. 1. As with the Ga islands, emission from such defects can shift by varying energies depending on the equilibrium distribution of band bendings beneath the defects. Finally, laser-excited defect states also probably contribute to emission in the upper part of the gap in Fig. 1.

Figure 2 displays data from angle scans made to verify the origin of the excited-state band. In Fig. 2(a) the sample is rotated about the  $\bar{\Gamma}$ - $\bar{X}'$  ([100]) direction by an angle  $\theta$ . The sketch illustrates the relationship between the annular aperture of the CMA and the surface BZ. In this case the entire annulus was open, giving a  $\phi$ -integrated EDC. The aperture limits the  $\theta$ -resolution to  $\pm 6^\circ$ . A peak around  $\theta = 35^\circ$  is evident in Fig. 2(a), in good agreement with the value of  $36^\circ$  calculated assuming that  $k_{\parallel}$  is conserved and that the electron affinity of the  $\bar{X}$  state is 4 eV. Note that there is significant excited-state photo-

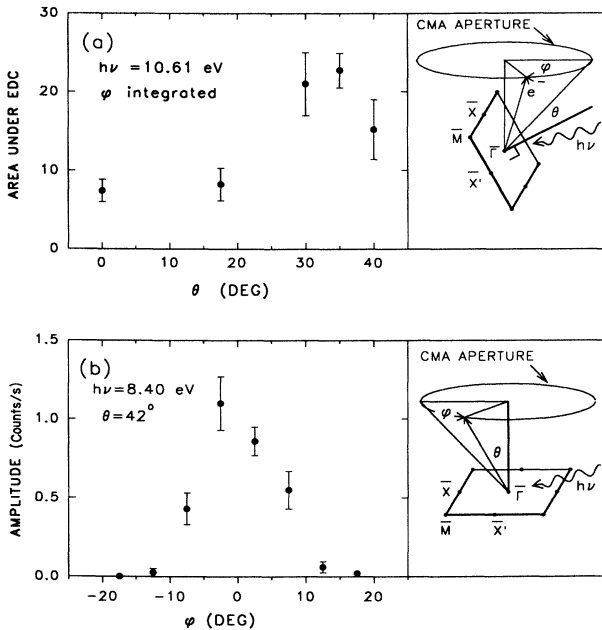


FIG. 2. Angular dependence of the photoemission from the  $\bar{X}$  state. Error bars denote counting statistics.

emission at  $\theta=0$  from states near the CBM. Its origin can be either the CBM or a surface state near  $\bar{\Gamma}$ .<sup>3</sup> This region of  $k$  space was not explored in detail.

Figure 2(b) shows a scan in which  $\theta$  is set for maximum  $\bar{X}$  emission at  $h\nu=8.40$  eV and  $\phi$  is varied by inserting into the CMA a rotatable aperture which restricts  $\phi$  to  $\phi\pm6^\circ$ . The  $p$ -polarized SR was incident at  $15^\circ$  grazing, which enhanced the absolute count rate relative to the more normal-incidence geometry of Fig. 2(a). The scan follows approximately the  $\bar{X}-\bar{M}$  direction in the BZ near  $\bar{X}$ , and reveals a resolution-limited peak corresponding to the  $k_{\parallel}$  of  $\bar{X}$ . In Fig. 2, as well as Figs. 3 and 4, a normalization to zero laser dose (defined as the incident fluence per pulse times the number of pulses) has been applied to the data to correct a dose-dependent decrease in the  $\bar{X}$  emission, discussed below.

EDC's for the  $\bar{X}$  excited state at various probe photon energies are presented in Fig. 3. Four of the EDC's were measured from a single cleave in the configuration of Fig. 2(a) with  $\theta$  adjusted with  $h\nu$  to follow the  $\bar{X}$  direction. The EDC for  $h\nu=8.40$  eV is from a different crystal in the grazing-incidence geometry of Fig. 2(b) and has been scaled arbitrarily. The inset plots the first moment of each EDC (and an additional EDC not shown) as a function of  $h\nu$ . The linear variation with unit slope is as anticipated for photoelectrons originating from a localized  $k$ -space minimum exhibiting no dispersion. The peak-count rates follow approximately the variation of the SR transmission through the LiF filter. At the present level of detail there appears to be no variation due to final-state effects. This is not surprising, since the band structure derived from ARPES (Ref. 14) indicates that, in order to intersect bulk bands having  $k$  components appropriate

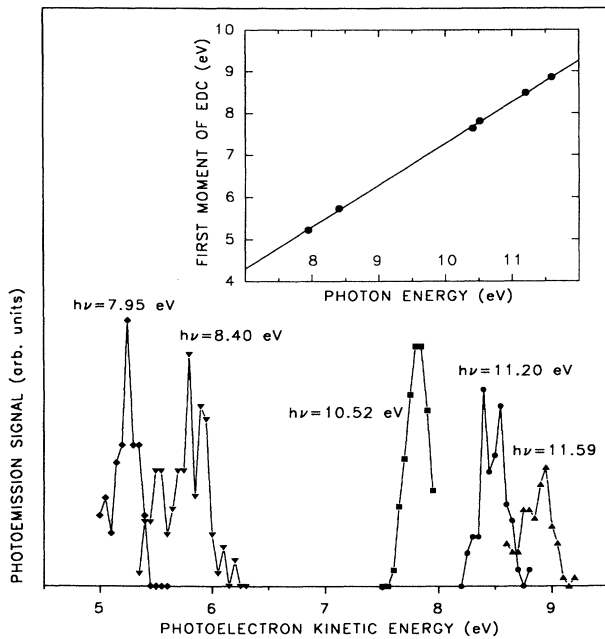


FIG. 3. Dependence of the laser-populated  $\bar{X}$  signal on the synchrotron photon energy  $h\nu$ , up to the LiF cutoff. The 8.4-eV EDC is scaled arbitrarily.

for final-state resonances, one would need  $h\nu \gtrsim 11$  eV, a range which barely overlaps the LiF transmission window.

The temporal evolution of the  $\bar{X}$  state is illustrated in Fig. 4. The solid curve is the measured laser-pulse profile. The data points represent areas beneath the  $\bar{X}$  photoemission band as a function of delay between the 0.5-ns probe SR pulse and the laser pulse. The open symbols required an amplitude correction for the laser-dose dependence but the solid symbols did not. The apparent time shift between pump profile and  $\bar{X}$  population indicates a decay time  $\lesssim 2$  ns, comparable to the expected lifetime of conduction electrons. This suggests that  $\bar{X}$  is effectively in equilibrium with the CBM population throughout the time decay. The earlier laser pump-probe data were consistent with  $\bar{X}$ -CBM equilibrium on picosecond time scales, although at higher electron densities.<sup>3</sup> Adopting the supposition of equilibrium, we depict with a dashed curve in Fig. 4 the bulk carrier density at the surface calculated by convolving an appropriate linear-response function with the laser pulse. Carrier diffusion, pump-laser absorption depth, and both bulk and surface recombination rates are all incorporated. For the conditions of these experiments, recombination can be approximated by an effective rate  $\tau_{\text{eff}}^{-1} \approx \tau^{-1} + s/d$ , where  $\tau$  is the bulk lifetime,  $d = (D\tau)^{1/2}$  is the carrier diffusion depth,  $D$  is the diffusion constant, and  $s$  is the surface recombination velocity. For the dashed curve of Fig. 4,  $\tau_{\text{eff}} = 1.3$  ns. The data do not allow the separate evaluation of  $\tau$  and  $s$ .

Although pump fluences for this work and for the picosecond laser experiment<sup>3</sup> are comparable,  $\sim 10^{15}$  photons/cm<sup>2</sup>, the peak electron densities [ $1 \times 10^{18}$  cm<sup>-3</sup> and  $(1-3) \times 10^{19}$  cm<sup>-3</sup>, respectively] and temporal ranges are much different. Nevertheless, if  $\bar{X}$ -CBM equilibrium is assumed, we find that the measured  $\bar{X}$  signal levels relative to the valence band are consistent between the two experiments. Thus the different pump photon energies in the two experiments, 2.43 (this work) and 1.72 eV (Ref. 3), neither of which can pump  $\bar{X}$  directly,<sup>7</sup> appear equally effective in populating  $\bar{X}$ . This is consistent with  $\bar{X}$  being populated indirectly via electron scattering. The question of equilibrium at long times and low densities is

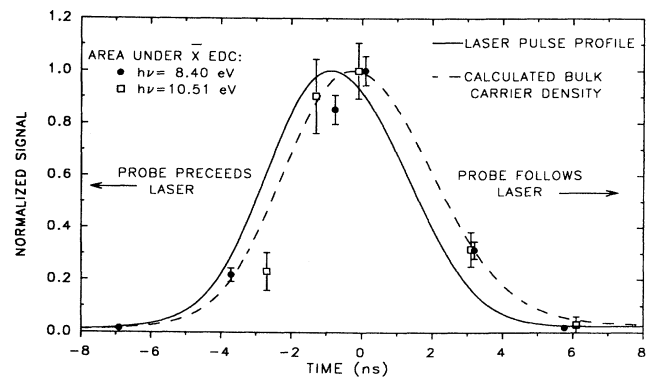


FIG. 4. Dependence of the  $\bar{X}$  signal intensity on the delay time between the laser pump and the synchrotron probe.

significant because, if the occupied  $\bar{X}$  state were several  $kT$  or more below the CBM, the populations could become decoupled at low electron densities.

The gradual decrease in the  $\bar{X}$  signal with laser dose mentioned above is probably not due to a reduction in the effective  $\bar{X}$  density of states because core-level spectra indicate that the surface-bonded Ga atoms, the orbitals of which give rise to the unoccupied surface state, decrease by at most 20% (Ref. 9) while the  $\bar{X}$  signal can fall by 70%. There are at least three alternative explanations, each of which is consistent with a small degree of laser-induced surface disruption: a spreading of the angular distribution if  $k_{\parallel}$  becomes less sharply defined because of the increased initial-state localization to be expected on a disordered surface; a decrease in the lifetime of  $\bar{X}$  electrons themselves through the creation of new recombination defects; or a decrease in bulk electron concentration as a consequence of increased surface recombination.

The present work is significant primarily as a successful first step in the use of tunable SR to probe laser-

excited states in semiconductors. The capability of this technique can be substantially improved with more suitable electron energy analyzers such as time of flight, with pump lasers having shorter pulses and higher repetition rates, and with a wider range of SR tunability. Using radiation from an undulator or a free-electron laser rather than a bending magnet can yield significant improvements in signal level and, for some laser and storage-ring combinations, in temporal resolution. Furthermore, these sources might enhance the tunability relative to the broad-band emission from a bending magnet because second order can be made small prior to monochromatization.

We wish to acknowledge useful conversations with J. C. Rife and R. Haight. This research was carried out in part at the National Synchrotron Light Source, which is sponsored by the U.S. Department of Energy under Contract No. DE-AC02-76CH00016.

<sup>1</sup>R. T. Williams, J. P. Long, and M. N. Kabler, *Opt. Eng.* **28**, 1085 (1989).

<sup>2</sup>N. J. Halas and J. Bokor, *Phys. Rev. Lett.* **62**, 1679 (1989).

<sup>3</sup>R. Haight and J. A. Silberman, *Phys. Rev. Lett.* **62**, 815 (1989).

<sup>4</sup>J. Bokor, R. Haight, R. H. Storz, J. Stark, R. R. Freeman, and P. H. Bucksbaum, *Phys. Rev. B* **32**, 3669 (1985).

<sup>5</sup>R. T. Williams, T. R. Royt, J. C. Rife, J. P. Long, and M. N. Kabler, *J. Vac. Sci. Technol.* **21**, 509 (1982).

<sup>6</sup>D. Straub, M. Skibowski, and F. J. Himpsel, *Phys. Rev. B* **32**, 5237 (1985); B. Reihl, T. Riesterer, M. Tschudy, and P. Perfetti, *ibid.* **38**, 13 456 (1988).

<sup>7</sup>Xuejun Zhu, S. B. Zhang, Steven G. Louie, and Marvin L. Cohen, *Phys. Rev. Lett.* **63**, 2112 (1989).

<sup>8</sup>J. P. Long, *Nucl. Instrum. Methods Phys. Res., Sec. A* **266**, 672 (1988).

<sup>9</sup>J. P. Long, S. S. Goldenberg, and M. N. Kabler, *Phys. Rev.*

*Lett.* **68**, 1014 (1992).

<sup>10</sup>J. P. Long, H. R. Sadeghi, J. C. Rife, and M. N. Kabler, *Phys. Rev. Lett.* **64**, 1158 (1990).

<sup>11</sup>Detailed calculations indicate that, in addition to bulk screening, and unlike the case of Si in Ref. 10, the charge on excited defect states must be contributing significantly to the SPV for these surfaces.

<sup>12</sup>S. S. Goldenberg, J. P. Long, and M. N. Kabler, in *Surface Chemistry and Beam-Solid Interactions*, edited by H. Atwater, F. A. Houle, and D. Lowndes, MRS Symposia Proceedings No. 201 (Materials Research Society, Pittsburgh, 1991), p. 519.

<sup>13</sup>R. Haight and J. Bokor, *Phys. Rev. Lett.* **56**, 2846 (1986).

<sup>14</sup>G. P. Williams, F. Cerrina, G. J. Lapeyre, J. R. Anderson, R. J. Smith, and J. Hermanson, *Phys. Rev. B* **34**, 5548 (1986).